*Journal of Applied Mechanics and Technical Physics, Vol. 45, No. 6, pp. 902–914, 2004*

# MODELING OF ENERGY ABSORPTION IN STEEL DURING ITS TREATMENT BY POWERFUL HIGH-FREQUENCY PULSES OF VARIED FREQUENCY

**V. G. Shchukin and V. V. Marusin**

UDC 621.785

*Based on the previously developed model of thermal, electromagnetic, and structural-phase processes in surface layers of carbon steels under the action of high-frequency pulses, the heat release in these layers in the range of allowable field frequencies from* 66 kHz *to* 40.12 MHz *is studied. The specific energy flux of the electromagnetic field is considered as the basic energy parameter characterizing the intensity of high-frequency treatment. Frequency dependences of the dynamics of steel heating up to the liquidus point for treatment regimes important for practice with* $\langle W \rangle = 10^8$ *and* $2 \cdot 10^8$ W/m$^2$ *for the width of the pulse-action zone on the steel surface equal to* 1.5 *and* 4 mm *are obtained. The data of numerical calculations are used to construct the specific flux of energy as a function of the maximum surface temperature; together with the results of numerical simulations of structural-phase transformations in the steel grain, these dependences allow one to choose the optimal hardening modes at different frequencies.*

**Key words:** *high-frequency pulse heating, steel, phase transformations, simulation.*

**Introduction.** Induction heating is widely used in modern industry in such operations as metal hardening, preheating in molding and soldering, etc. The classical methods of induction heating (high-frequency current methods [1]) are characterized by comparatively moderate current densities, which ensure the specific energy-release power of the order of $\langle W \rangle = 10^6$–$10^7$ W/m$^2$; however, the transition to the pulse mode is characterized by an increase in $\langle W \rangle$ up to $10^9$ W/m$^2$. The drastic decrease in treatment time justifies the use of inductor currents of much higher frequency (about 1 MHz and higher), whereas the frequency for conventional methods is within 200 kHz. Several recent papers deal with the development of particular technologies of obtaining and experimental investigation of the structure of thin hardened steel layers under the action of electromagnetic field pulses with a frequency above 1 MHz [2–6]. Nevertheless, this problem has not been adequately studied theoretically.

This complicated problem includes electromagnetic, thermal, and structural-phase phenomena. Planning and experimental investigation of the system of pulse induction heating usually require a series of expensive and long-time experiments (the research results obtained during 12 years are analyzed in [2]). For this reason, numerical simulations become more important. Until now, numerical simulations of induction heating were limited to moderate field frequencies ($f$ = 10–200 kHz) acting on steel specimens of an axisymmetric [7–9] or planar form [10].

The authors have previously developed a model of local treatment of carbon steel by short single pulses of a high-frequency electromagnetic field and performed a series of calculations with $f$ = 440 kHz [11]. Based on the model of [11], numerical simulations of induction treatment of steel were performed in a wide range of field frequencies: from 66 kHz to 40 MHz. The calculations were performed for all allowable frequencies above 440 kHz, namely, 1.76, 5.28, 13.5, 27.1, and 40.12 MHz. The study was aimed at finding the dependences between the energy parameters of the treatment processes and the size of the hardened zone (i.e., zone with a changed phase

Institute of Theoretical and Applied Mechanics, Siberian Division, Russian Academy of Sciences, Novosibirsk 630090; marusin@itam.nsc.ru. Translated from Prikladnaya Mekhanika i Tekhnicheskaya Fizika, Vol. 45, No. 6, pp. 154–168, November–December, 2004. Original article submitted June 17, 2003; revision submitted February 4, 2004.

 

composition) in a given frequency range. The basic energy parameter characterizing the intensity of high-frequency (HF) treatment was assumed to be the specific flux of energy of the electromagnetic field $\langle W\rangle$ averaged over the pulse duration and area of the field-action zone on the metal surface. The numerical experiments were limited to those regimes of pulse induction heating for which the value of $\langle W\rangle$ by the end of the pulse action is approximately $\langle W\rangle_1 = 10^8$ W/m$^2$ and $\langle W\rangle_2 = 2\cdot 10^8$ W/m$^2$, which are most typical values in the technological aspect [2–6]. In addition, the calculated data were compared with available experimental results on specific energy absorption for a given period of time and hardened layer depth.

**Formulation of the Problem and Description of the Mathematical Model.** We consider the action of a high-frequency pulse on a massive steel specimen. The area of action of the transverse electromagnetic field is localized in a narrow region on the specimen surface (by using ferrite magnetic screens, choosing a specific shape of the inductor, etc.). If the vector of current in the inductor is directed along one Cartesian coordinate, then, in formulating the mathematical problem, we can confine ourselves to consideration of processes in the specimen cross section perpendicular to the direction of current in the inductor. In this case, the computational domain limiting the entire region of the thermal action in the steel specimen is a rectangle with the sides $2L_x$ and $L_y$, such that $X\in[-L_x, L_x]$, $Y\in[0, L_y]$, $L_y < L_x$, where the $X$ coordinate is directed along the specimen surface and the $Y$ coordinate is directed perpendicular to the $X$ coordinate inward the specimen. The origin of the computational domain is located at the point $(0, 0)$ corresponding to the projection of the central axis of the working surface of the inductor. The width of this working surface is $2L_i$ ($L_i \ll L_x$).

Let us consider the system of equations of the self-consistent model of thermal, electromagnetic, and structural-phase phenomena in the working region [11]. We assume that the characteristic size is the thickness of the skin layer of steel at the Curie point

$$\Delta_{\rm C} = [2\rho_{\rm C}/(\omega\mu_0)]^{1/2},$$

and the characteristic time is the time of heating due to Joule losses in a layer of thickness $\Delta_{\rm C}$ from the initial temperature $T_0$ to the iron melting point $T_{\rm m} = 1800$ K under the condition that the decrease in amplitude of the magnetic field strength from the maximum on the surface $H_{\max}$ to zero at the depth of the skin layer is linear:

$$t_* = \gamma_{\rm C} C_{\rm C}\Delta T_{\rm m}\Delta_{\rm C}^2/(\rho_{\rm C}H_{\max}^2) = 2\gamma_{\rm C}C_{\rm C}\Delta T_{\rm m}/(\omega\mu_0 H_{\max}^2).$$

Here $\gamma$ is the specific weight of steel, $\rho$ is the specific resistance of steel, $C$ is its specific heat capacity, $\omega = 2\pi f$ ($f$ is the generator frequency), and $\mu_0$ is the magnetic constant; the subscript C indicates that the parameter corresponds to the Curie temperature $T_{\rm C} = 1043$ K. This method of determining the characteristic time is preferable as compared to the commonly accepted method, where the characteristic time is determined in terms of thermal diffusivity $\chi$ (e.g., $t_{*1} = \Delta_{\rm C}^2/\chi_{\rm C} = \gamma_{\rm C}C_{\rm C}\Delta_{\rm C}^2/\lambda_{\rm C}$, where $\lambda$ is the thermal conductivity) because it yields the values of $t_*$ commensurable with the treatment-pulse duration $t_i$, whereas $t_{*1} \gg t_i$.

By substituting the variables $x = X/\Delta_{\rm C}$, $y = Y/\Delta_{\rm C}$, and $\tau = t/t_*$ and introducing the relative transport coefficients normalized to their values at the Curie point ($\bar\gamma = \gamma/\gamma_{\rm C}$, $\bar\rho = \rho/\rho_{\rm C}$, etc.), the relative temperature $\theta = (T - T_0)/\Delta T_{\rm m}$, and the vector of relative strength of the magnetic field $\boldsymbol{h} = (h_x, h_y)$, where $h_x = H_x/H_{\max}$ and $h_y = H_y/H_{\max}$, we obtain the following dimensionless equations for heat conduction and electromagnetic field (in a complex form) in the steel-specimen cross section:

$$\bar\gamma\bar c\,\frac{\partial\theta}{\partial\tau} = \frac{1}{K_H}\Big(\frac{\partial}{\partial x}\,\bar\lambda\,\frac{\partial\theta}{\partial x} + \frac{\partial}{\partial y}\,\bar\lambda\,\frac{\partial\theta}{\partial y}\Big) + p(x, y, \tau); \tag{1}$$

$$\frac{\partial}{\partial x}\,\bar\rho\,\frac{\partial h_y}{\partial x} - \frac{\partial}{\partial x}\,\bar\rho\,\frac{\partial h_x}{\partial y} = 2j\mu h_y; \tag{2}$$

$$\frac{\partial}{\partial y}\,\bar\rho\,\frac{\partial h_x}{\partial y} - \frac{\partial}{\partial x}\,\bar\rho\,\frac{\partial h_y}{\partial y} = 2j\mu h_x. \tag{3}$$

Here

$$p(x, y, \tau) = \bar\rho|\operatorname{rot}\boldsymbol{h}|^2 = \bar\rho\Big[\Big(\frac{\partial\operatorname{Re}h_y}{\partial x} - \frac{\partial\operatorname{Re}h_x}{\partial y}\Big)^2 + \Big(\frac{\partial\operatorname{Im}h_y}{\partial x} - \frac{\partial\operatorname{Im}h_x}{\partial y}\Big)^2\Big]$$

is the dimensionless volume density of energy release and $K_H = \rho_{\rm C}H_{\max}^2/(\lambda_{\rm C}\Delta T_{\rm m})$ is a dimensionless parameter approximately equal to the ratio of the maximum flux of magnetic energy to the conductive heat flux at the Curie

temperature. The greater $K_H$, the less significant the contribution of heat-conduction processes as compared to the Joule sources of heating. In particular, for $H_{\max} \approx 10^5$ A/m, $\lambda_{\rm C} = 30$ W/(m·K), $\rho_{\rm C} = 1.2$ $\mu\Omega\cdot$m, and $\Delta T_{\rm m} = T_{\rm m} - T_0 = 1800 - 300 = 1500$ K, we obtain $K_H \approx 0.25$.

Equations (1)–(3) have to be solved under the boundary conditions

$$\theta(x,y,\tau)\Big|_{x=\pm l_x} = \theta(x,y,\tau)\Big|_{x=l_y} = \theta(x,y,0) = 0,$$

$$\bar\lambda\,\frac{\partial\theta(x,y,\tau)}{\partial y}\Big|_{y=0} = \bar\alpha^T\theta(x,y,\tau)\Big|_{y=0},$$

$$h_x(\pm l_x,y) = h_y(\pm l_x,y) = h_x(x,l_y) = h_y(x,l_y) = 0;$$

$$h_x(x,0) = f_1(x), \qquad h_y(x,0) = f_2(x), \tag{4}$$

where $l_x = L_x/\Delta_{\rm C}$, $l_y = L_y/\Delta_{\rm C}$, $\bar\alpha^T = (\Delta_{\rm C}/\lambda_{\rm C})\{\alpha^T + \sigma[T(x,0,t)+T_0][T^2(x,0,t)+T_0^2]\}$, $\alpha^T$ is the heat-transfer coefficient from the specimen surface, $\sigma$ is the Stefan–Boltzmann constant, and $f_1(x)$ and $f_2(x)$ are known functions defining the field distribution on the specimen surface.

The kinetics of carbon redistribution in an individual grain of hypoeutectoid steel consisting initially of pearlite and ferrite subgrains with an effective radius $R_{\rm g}$ is described by the equation of austenite-phase growth (first, in the central pearlite grain of effective radius $R_{\rm p}$, and then in the ambient excess ferrite) and by the equation of diffusion transport of carbon in the austenite phase [11], which are solved together with the equations of the thermal problem (1)–(3) only at those points of the computational domain that have the temperature higher than the point of the beginning of decomposition of the initial structure $Ac_1 = 1000$ K. In particular, at the stage of complete transformation of the pearlite grain to austenite [when the effective radius of the austenite grain $R_{\rm a}$ becomes greater than the effective initial radius of the pearlite grain $R_{\rm p}$ related to the initial grain size of St. 45 steel as $R_{\rm p} = R_{\rm g}(0.45/0.8)^{1/3} = 0.825R_{\rm g}$], one has to solve, first, the unsteady equation of carbon diffusion in the grain with allowance for its spherical symmetry

$$\frac{\partial C(r,\tau)}{\partial\tau} = \frac{t_*}{r^2}\,\frac{\partial}{\partial r}\,r^2D(\theta)\,\frac{\partial C(r,\tau)}{\partial r}, \qquad 0 \leqslant r \leqslant R_{\rm a}(\tau), \tag{5}$$

and, second, in the temperature range $\theta_1 < \theta < \theta_2$ [$\theta_1 = (Ac_1 - T_0)/\Delta T_{\rm m}$ and $\theta_2 = (Ac_3 - T_0)/\Delta T_{\rm m}$, where $Ac_1 = 1000$ K and $Ac_3 = 1185$ K are the initial and final points of the phase transformation, respectively], the equation of kinetics of the volume fraction of austenite $f^a(\tau) = [R_{\rm a}(\tau)/R_{\rm g}]^3$ in the grain:

$$\frac{df^a}{d\tau} = \frac{D(\theta)(f^a)^{2/3}t_*}{R_{\rm g}a_0}\Big[1 - \exp\Big(-\frac{L_{\rm a}(\theta-\theta_1)}{R\theta\theta_1\Delta T_{\rm m}}\Big)\Big]. \tag{6}$$

The initial conditions for Eqs. (5) and (6) are formulated with allowance for the initial structure of steel:

$$C(r,0) = \begin{cases} C_{\rm eut} = 0.8, & 0 \leqslant r \leqslant R_{\rm p}, \\ 0, & R_{\rm p} < r \leqslant R_{\rm a}, \end{cases} \qquad f^a(0) = f_0^p.$$

Equations (5) and (6) are closed by the condition of symmetry at the center of the grain and by the equation of conservation of mass for carbon in the grain (St. 45 steel):

$$\frac{1}{r}\,\frac{\partial C}{\partial r}\Big|_{r=0} = 0, \qquad 3\int\limits_0^{R_{\rm a}} r^2C(r)\,dr = 0.45R_{\rm g}^3.$$

Here $f_0^p = (R_{\rm p}/R_{\rm g})^3$ is the initial fraction of the pearlite phase in steel, $a_0$ is the iron-lattice constant, $L_{\rm a}$ is the latent heat of phase transformation, $D(\theta)$ is the temperature dependence of carbon diffusivity in steel, and $D(\theta) = A(\theta)\exp[-B(\theta)]$. The following values of parameters for St. 45 steel were used in calculations: $R_{\rm g} = 2\cdot10^{-5}$ m, $f_0^p = 0.5625$, $a_0 = 2.9\cdot10^{-10}$ m, $L_{\rm a} = 16.1\cdot10^3(0.67-\theta)$ J/mole, $A(\theta) = 4.53\cdot10^{-7}(1+0.098/\theta)$ m$^2$/sec, and $B(\theta) = 9.58/\theta - 3.82$ [11].

We ignore the change in temperature over the grain radius and assume it to be equal to the value at the point of the surface layer with the coordinates $x$ and $y$:

$$\theta(r,\tau) = \theta(x,y,\tau), \qquad 0 \leqslant r \leqslant R_{\rm g}.$$

The present study differs from the calculations in [11] by the choice of the boundary conditions (4) for solving the electromagnetic problem (2), (3), i.e., by the choice of the functions $f_1(x)$ and $f_2(x)$. To avoid a possible discontinuity in calculating partial derivatives of the amplitude of magnetic field strength at the boundaries of the region of its action and, as a consequence, a discontinuity in the energy-absorption estimate $p(x, y, \tau)$ in (1), the real parts of the complex components of the strength vector $h_x$ and $h_y$ and the absolute value of the latter $h_S = \sqrt{|h_x(x,0)|^2 + |h_y(x,0)|^2}$ on the surface $y = 0$ are set as follows:

$$\operatorname{Re} h_x(x,0) = \frac{1}{1+\exp\left((|x|-x_{10})/\delta_1\right)},$$

$$h_S(x,0) = \frac{1}{1+\exp\left((|x|-x_{20})/\delta_2\right)}, \qquad \operatorname{Re} h_y(x,0) = \sqrt{h_S^2(x,0) - [\operatorname{Re} h_x(x,0)]^2}.$$

In this case, the functions $\operatorname{Re} h_x$ and $\operatorname{Re} h_y$ decrease exponentially as $|x| \to \infty$, and their derivatives with respect to the $x$ coordinate are continuous and bounded. The imaginary parts $\operatorname{Im} h_x$ and $\operatorname{Im} h_y$ are equal to zero for $y = 0$. The approximation parameters $\delta_1^* = \delta_1 \Delta_{\mathrm{C}}$, $\delta_2^* = \delta_2 \Delta_{\mathrm{C}}$, $X_{10} = x_{10}\Delta_{\mathrm{C}}$, and $X_{20} = x_{20}\Delta_{\mathrm{C}}$, which define, respectively, the "steepness" of the amplitude decrease near the center and the width of the zone with the maximum strength, are mainly related to the geometric parameter $L_i$. They were estimated by the results of an approximate analytical solution of the problem of the surface-current distribution [12]. In all calculation variants, $\delta_1^* = \delta_2^* = 0.2L_i$, $X_{10} = 1.14L_i$, and $X_{20} = 1.52L_i$.

The experimentally measured characteristic of induction heating is the specific energy flux in the zone of action of the field [2, 3], because it is impossible to directly measure the field strength in the specimen. If the half-width of the working region of the inductor is $L_i$ and the duration of the HF pulse is $t$, the specific energy flux in this region on the specimen surface averaged over the time interval $[0, \tau = t/t_*]$ is

$$\langle W \rangle(\tau) = \frac{\rho_{\mathrm{C}} H_{\max}^2}{2L_i\tau} \int\limits_{-l_x}^{l_x} \int\limits_{0}^{l_y} \int\limits_{0}^{\tau} p(x,y,\tau)\, dx\, dy\, d\tau. \tag{7}$$

The experimental values of $\langle W \rangle$ measured at the corresponding field frequency $\omega$ and pulse duration $t$ being available, we construct the following numerical algorithm. With an arbitrarily chosen $H_{\max}$, we solve system (1)–(3), (5), (6) with appropriate boundary conditions over the entire time interval, then we find the next approximation for $H_{\max}$ from Eq. (7), etc. When the necessary degree of convergence of the calculated value of $\langle W \rangle$ to its *a priori* prescribed value is reached, we obtain the distributions of temperature, volume fraction of austenite, and concentration of carbon in the latter over the steel-specimen cross section for such a maximum amplitude of field strength at the central point of the surface $H_{\max}$ that ensures a specified energy contribution during pulse HF treatment.

**Numerical Inspection of the Model and Discussion of the Results Obtained.** The proposed model with $f = 440$ kHz and implicit difference schemes used for its approximation were inspected in detail in [11], where satisfactory agreement of numerical and experimentally observed dependences of the size of the hardened region on the specific power and pulse duration was reached. At the same time, there is no sufficient knowledge for higher field frequencies, though there are some data on the use of induction quenching of metals at frequencies $f > 1$ MHz. Stahli [2] reviewed available experimental data and systematized them in a wide range of specific power and exposure time above the point of the beginning of steel austenization by treatment with electromagnetic pulses with a significantly higher frequency: $f = 27.1$ MHz.

It is difficult to verify workability of the proposed model on the basis of the data of [2] because the postulate of a constant amplitude of inductor current over the entire range of action of the HF pulse is not supported, the method of generation of HF pulses being different from that in [11]. We can only assume that an approximately exponential decrease in the current amplitude and, hence, energy flux on the steel-specimen surface occurs in accordance with the parameters of the oscillatory circuit in the generator. If we assume that the strength amplitude on the specimen surface obeys the dependence

$$H_{\max}(t) = H_0 \exp(-kt),$$

we can reasonably choose the parameter $H_0$ and the attenuation constant $k$ to obtain the ranges of specific energy absorption and durations of steel treatment close to those cited in [2]. Then, the adequacy of the model to actual

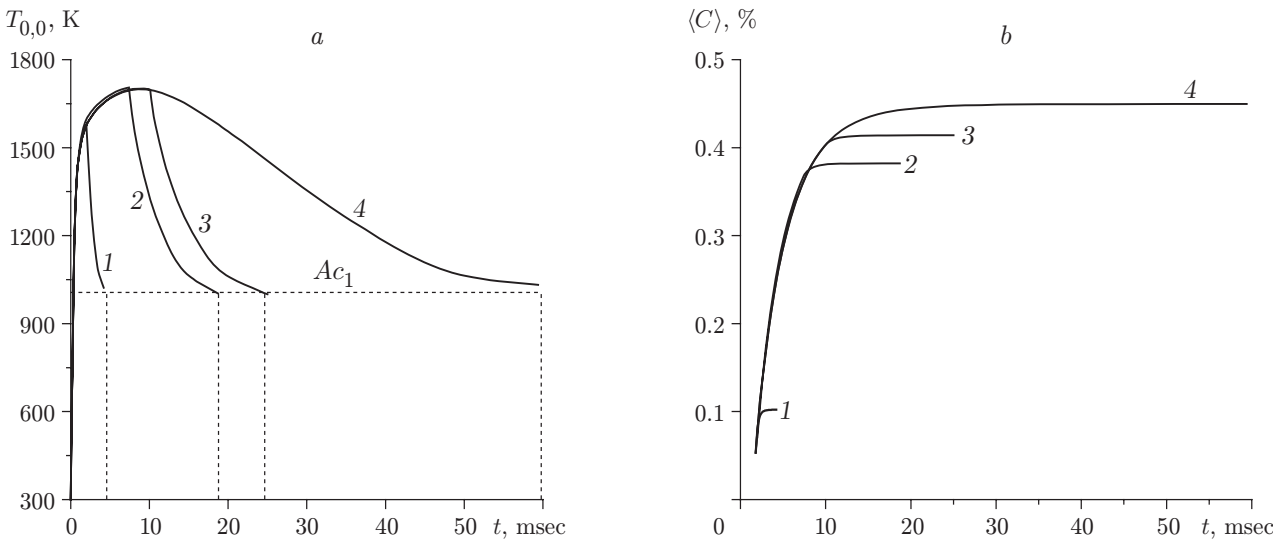


Fig. 1. Calculated changes in surface temperature at the center of the treatment zone (a) and mass fraction of carbon in this zone (b) for the field frequency $f = 27.1$ MHz and HF pulse duration of 2 (1), 7.5 (2), 10 (3), and 60 msec (4).

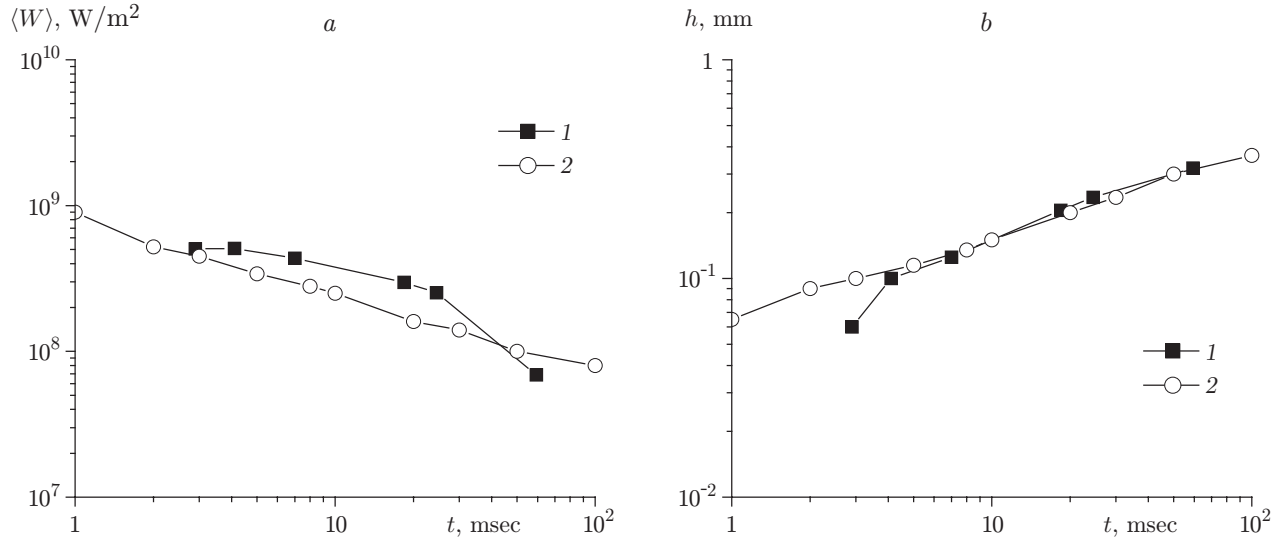


Fig. 2. Calculated (1) and experimental (2) values of the mean specific energy absorption (a) and hardening depth $h$ (b) for $f = 27.1$ MHz.

conditions of quenching is determined by the closeness of the calculated geometric parameters of the hardened region and their experimental estimates for the same treatment conditions.

The results of such a comparison for the hardening depth at the central point of the surface of the St. 45 steel specimen are plotted in Figs. 1 and 2. The following parameters were used in calculations: half-width of the working region of the inductor $L_i = 10$ mm, $H_0 = 1.7 \cdot 10^5$ A/m, and $k = 0.033$ sec$^{-1}$. To determine austenization duration, we calculated the entire treatment cycle, including the cooling stage. According to the calculations, the maximum surface temperature does not exceed 1700 K for the entire range of pulse duration from 2 to 60 msec. As the hardening depth $h$, we used the isoline of equal concentrates 0.05, which corresponds to the beginning of noticeable decomposition of pearlite when the mean mass content of carbon in ferrite interlayers reaches 0.05%.

TABLE 1

Parameters of Induction Treatment

| Working frequency of the generator $f$, MHz | Specific power $\langle W \rangle$ | | | |
|---|---|---|---|---|
| | $\langle W \rangle = 10^8$ W/m$^2$ | | $\langle W \rangle = 2 \cdot 10^8$ W/m$^2$ | |
| | $2L_i = 1.5$ mm | $2L_i = 4.5$ mm | $2L_i = 1.5$ mm | $2L_i = 4.5$ mm |
| 0.066 | 3.6/197/3.6 | 3.4/220/3.1 | 6.5/62/11.4 | 6.3/65/10.6 |
| 0.440 | 2.3/77/1.36 | 2.4/69/1.5 | 3.6/30/3.45 | 3.7/28/3.7 |
| 1.76 | 2.0/24/1.06 | 1.9/28/0.94 | 2.55/15/1.72 | 2.50/16/1.66 |
| 5.28 | 1.5/14/0.6 | 1.4/16/0.53 | 2.08/7.6/1.15 | 2.06/7.7/1.14 |
| 13.5 | 1.17/9.3/0.36 | 1.14/9.8/0.35 | 1.76/4.1/0.83 | 1.73/4.3/0.8 |
| 27.1 | 0.94/7.2/0.23 | 0.96/6.9/0.24 | 1.5/2.8/0.6 | |
| 40.12 | 0.91/5.2/0.22 | 0.87/5.0/0.2 | 1.3/2.4/0.47 | |

**Note.** The table gives the values of $H_{\max} \cdot 10^5/t_*/K_H$ ($H_{\max}$ in A/m and $t_*$ in msec).

For $f = 27.1$ MHz, the agreement of numerical data and experimental results of [2] is fairly satisfactory, especially for the hardening depth. Since good agreement was also obtained for the field frequency $f = 440$ kHz [11], we can cautiously assume that the simulation results will be in agreement with experimental data (for the same geometry of the working region) within the entire range of field frequencies from 66 kHz to 40.1 MHz.

The simulation parameters of pulse induction treatment of St. 45 steel are summarized in Table 1. As the frequency increases, the amplitude of magnetic field strength that ensures heating with an unchanged level of specific power decreases noticeably. This occurs because of the strong dependence of the metal skin-layer thickness on the field frequency. For a constant amplitude of alternating current in the inductor, the volume density of heat release in metal, as well as the Joule heat fluxes, rapidly increase with increasing field frequency. Therefore, to satisfy the condition of a constant mean power accepted in the model, we had to find the values of $H_{\max}$ corresponding to each regime of induction treatment by the method of consecutive approximations; these values are listed in Table 1. The criterion $K_H$ changes in proportion to $H_{\max}$, i.e., the contribution of conductive heat transfer, as compared to the flux of magnetic energy, becomes more significant with increasing frequency. As a result, the characteristic time of the process $t_*$ also decreases. As it follows from Table 1, the characteristic times with increasing frequency become less and less sensitive to variation of process parameters such as the mean power of energy absorption and the width of the region of field action: the difference in the values of $t_*$ is within 2–3 msec for $f > 20$ MHz and reaches several tenths of a second for $f = 66$ kHz.

Based on the tabulated data, we can conclude that the higher the field frequency, the more preferable the regime of pulse treatment as compared to the continuous regime with a moving source, since it is easier to ensure the necessary time parameters of the process in the first case.

The results of modeling of the heating–cooling dynamics in the range of chosen frequencies of electromagnetic pulses are analyzed below. The major part of calculations was performed on a grid containing $400 \times 200$ nodes in the longitudinal and normal to the body surface directions ($x$ and $y$, respectively). A sampling analysis of accuracy and convergence of data on a grid with a large number of nodes showed that the error in determining the temperature and concentration fields was less than $10^{-4}$, and the error in determining the electromagnetic field was $10^{-3}$. The calculation error largely depends on the field frequency. The time step $\Delta t$ was chosen depending on the heating rate so that the maximum change in temperature was within 50 K. The value of $\Delta t$ was varied from 1 to 0.1 msec in the entire range of $f$ and $\langle W \rangle$.

Let us consider the heating dynamics of the surface layer of steel with increasing field frequency. Figure 3 shows the calculated absolute temperature at the central point of the specimen surface as a function of dimensionless time. As it follows from the calculations, a gradual transition is observed in the chosen range of specific pulse power from the regime with a smooth decrease in the heating rate ($f = 66$ kHz) to the regime characterized by a sharp inflection of the temperature curve at a certain time and subsequent much slower heating ($f \geqslant 27.1$ MHz). The heating dynamics for intermediate values of the field frequency has a more complicated character (depending on the width of the zone of field action) caused by the nonlinear dependence of magnetic, thermal, and electrophysical properties of steel on temperature.

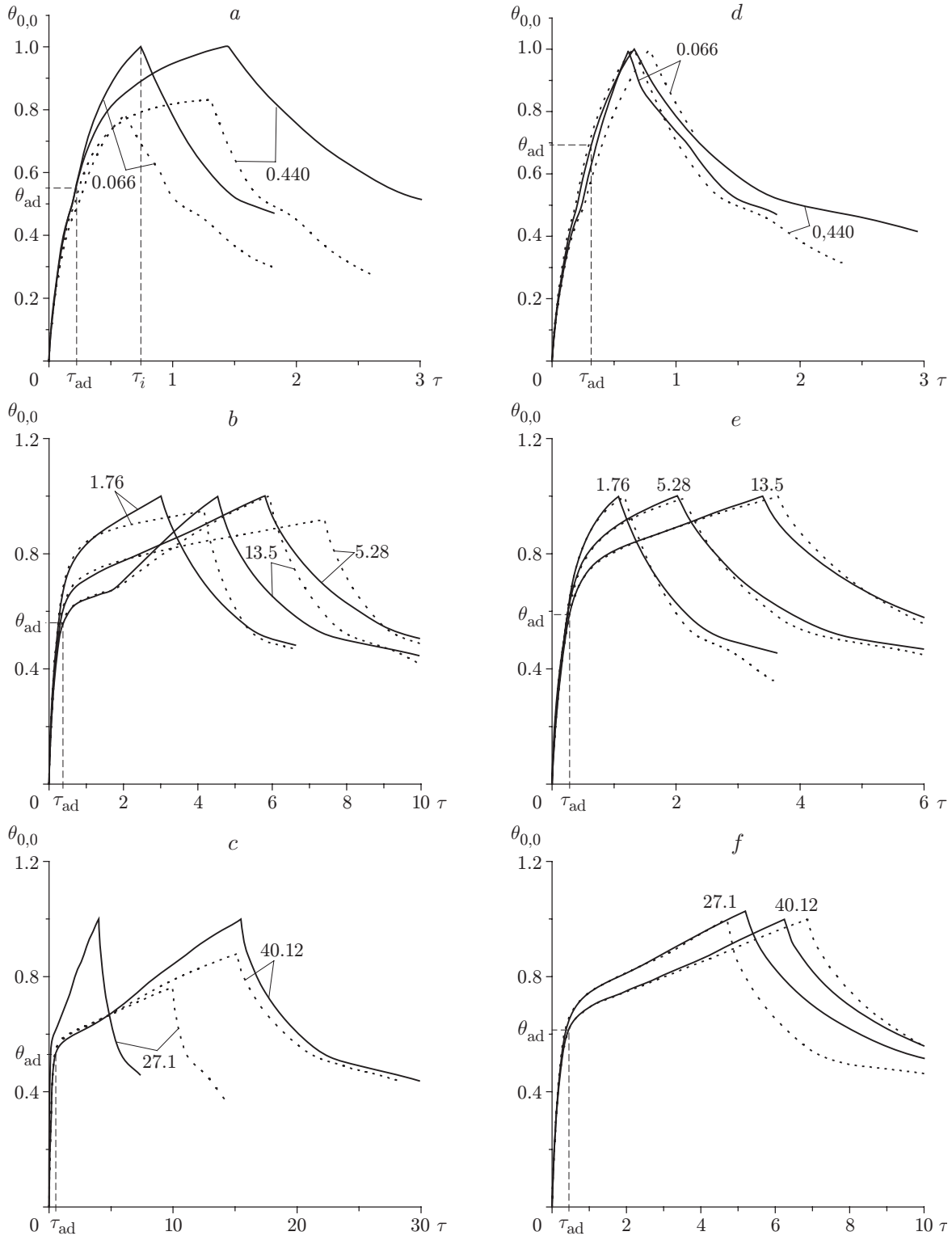


Fig. 3. Kinetics of steel heating in relative units at the central point of the surface for different values of the field frequency (the numbers at the curve indicate the frequency $f$ in MHz), heating-zone width, and mean energy absorption during a pulse for $\langle W\rangle = 10^8$ (a, b, and c) and $2\cdot 10^8$ W/m$^2$ (d, e, and f) and $2L_i = 1.5$ mm (dashed curves) and 4.5 mm (solid curves).

The specific feature of the curves obtained is their complete coincidence at the initial stage of heating. Until the time $t_{ad}$ approximately equal to one half of the characteristic time ($\tau_{ad} = t_{ad}/t_* = 0.25$–$0.5$), steel is heated with a maximum rate possible under given conditions. This stage of heating can be conventionally called quasi-adiabatic because of the minimum heat release from the zone of dissipation of energy of the electromagnetic field. The surface temperature at the center of the zone of field action at the time $\tau_{ad}$ depends weakly on treatment-mode parameters and reaches approximately 1200 K ($\theta_{ad} \approx 0.6$). Taking into account the nonuniformity of energy release along the abscissa axis, we can conclude that this temperature approximately corresponds to the time when the major part of the steel surface is heated above the Curie point ($T_C = 1043$ K and $\theta_C = 0.495$). The higher the pulse power, the greater the heating nonuniformity: the volume density of energy release at the center of the "heating spot" is significantly higher than that near the inductor exit, and peripheral regions are mainly heated due to heat addition from the central zone.

Expanding of the zone of field action $2L_i$ from 1.5 to 4.5 mm has practically no effect on the relative dynamics of surface heating at the initial stage: a small increase in the heating rate can be noticed only for a comparatively low frequency of the field (see Fig. 3a and d), but this factor becomes rather important in the entire range of frequencies at the later stage, when the major part of the surface layer is deprived of magnetic properties, at least if the pulse power is comparatively low (see Fig. 3b and c).

When high temperatures are reached ($\theta > \theta_{ad}$), the character of heating is primarily determined by the field frequency. The higher the frequency, the greater the decrease in specific power of heat release as compared to the period of initial heating. In the range of moderately high frequencies (66 and 440 kHz; Fig. 3a and d), the calculations demonstrate a smooth decrease in the heating rate because the volume energy-release density decreases monotonically with time in an inverse proportion to the increase in skin-layer thickness. As the frequency increases severalfold, the heating rate reaches a maximum and drastically decreases (almost by an order of magnitude); in the case of moderate values of the inductor width ($2L_i = 1.5$ mm) and pulse power ($\langle W \rangle = 10^8$ W/m$^2$), it can become so small that surface heating to a temperature of 1800 K close to the iron melting point can hardly be reached during the time of action of the HF pulse (the restriction $t_i \leqslant 100$–$200$ msec is caused by technical conditions). As was emphasized above, the transition to regimes of treatment with a higher frequency but with an unchanged mean power of energy release in steel is accompanied by a proportional decrease in amplitude of magnetic field strength (see Table 1), i.e., by an increase in relative magnetic permeability of steel in the initial state $\mu(T_0)$. In passing through the Curie point, steel loses its magnetic properties ($\mu = 1$), and the depth of field penetration increases proportionally to $\sqrt{\mu(T_0)}$; as a result, the mean energy-release density decreases by the same factor. The higher $\mu(T_0)$, the more significant the difference between the energy-release levels at a given cross-sectional point of steel in the initial state and upon heating above $T_C$. If the surface heating rate decreases so that heating to the melting point $T_m$ in a given range of admissible values of $t_i$ becomes impossible, the heating stage was terminated at a lower surface temperature (1500–1700 K).

At temperatures $\theta \gg \theta_{ad}$, the distribution of internal heat sources over the steel cross section becomes practically stabilized (the energy-release power is proportional to the ohmic resistance of steel, which increases very weakly at $\theta > \theta_C$). In contrast to heating at low frequencies, the following situation is observed with increasing frequency: after a period of comparatively slow heating during which temperature gradients in the surface layer become equalized, there follows a stage of regular heating with a higher constant heating rate up to the melting point (see Fig. 3b and c). As the pulse power increases, the stage of slow heating becomes almost unnoticeable (Fig. 3e and f).

In relative units, the time of heating up to 1800 K, i.e., the pulse duration $\tau_i$ (if possible), increases with increasing frequency: approximately from 0.75 for $f = 0.066$ MHz to 6–7 and 14–15 for $f = 40.12$ MHz and $\langle W \rangle = 2 \cdot 10^8$ and $10^8$ W/m$^2$, respectively. Thus, at elevated frequencies, conductive heat transfer of a very thin skin layer with the surrounding colder metal plays an important role only at the late stages of heating ($\tau > 1$), whereas its role is important during the entire pulse ($0 < \tau \leqslant \tau_i$) at low frequencies if the skin-layer thickness is commensurable with the characteristic length of heat conduction.

Figure 4 shows the specific power of energy release in steel as a function of the governing parameters of the process in the coordinates $\langle W \rangle$–$T$. At the lowest frequency ($f = 0.066$ MHz; Fig. 4a and d), the energy contribution to the steel specimen increases monotonically as steel is heated. At much higher field frequencies ($f = 1.76$ MHz and higher), however, the values of absorbed power, calculated by averaging over short intervals of heating, when

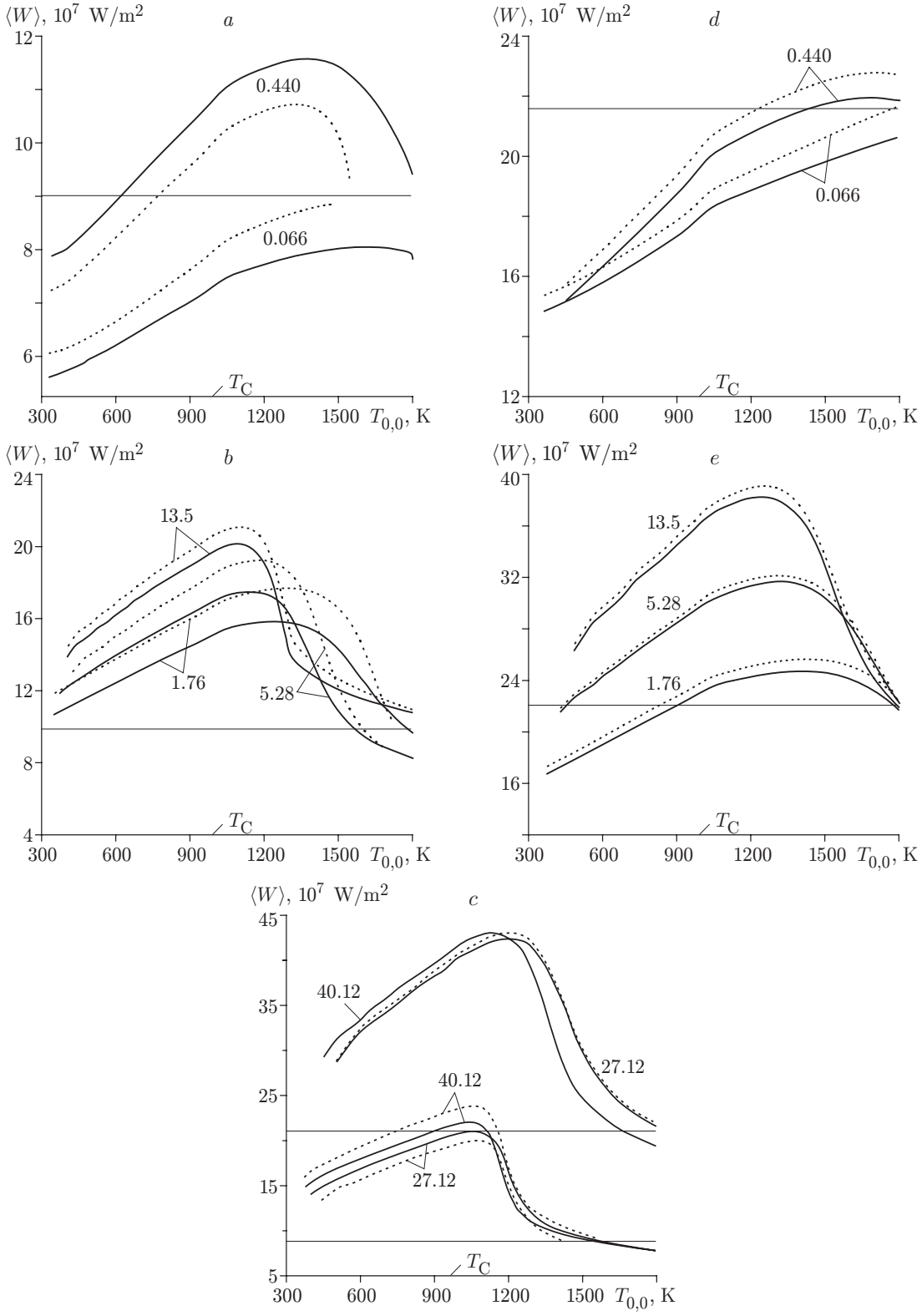


Fig. 4. Mean energy absorption versus the steel-surface temperature at the center of the "heating spot" for the heating zone width $2L_i = 1.5$ (dotted curves) and 4.5 mm (solid curves) and mean energy absorption during the entire pulse $\langle W \rangle = 10^8$ (a, b, and c) and $2 \cdot 10^8$ W/m$^2$ (b, d, and e).

the temperature at the center of the "spot" does not exceed 1200–1300 K, is higher than the values at the end of heating up to 1800 K by a factor of 1.5–2. Therefore, the value of $\langle W \rangle$ itself cannot serve as the energy characteristic of the process of high-frequency pulse quenching (HFPQ) if there are no data on the time framework of the process.

From the viewpoint of energy saving, regimes of induction pulse treatment of steel with the maximum value of $\langle W \rangle$ (other input parameters being identical) are most efficient. The calculation data show that regimes with heating up to temperatures within 1200–1500 K satisfy this criterion.

The efficiency of energy contribution can be most clearly demonstrated by means of the HFPQ efficiency $\eta$, which can be determined as the ratio of the amount of heat released during a certain time in the metal cross section with $2L_i$ and $\Delta_C$ to the total energy of the electromagnetic field released in the entire specimen during the same time:

$$\eta(\tau) = \frac{\int\limits_0^{\tau} \int\limits_{-l_i}^{l_i} \int\limits_0^1 \bar{\gamma}\bar{c}\,\dfrac{\partial\theta}{\partial\tau}\,d\tau\,dx\,dy}{\int\limits_0^{\tau} \int\limits_{-l_x}^{l_x} \int\limits_0^{l_y} p(x,y,\tau)\,d\tau\,dx\,dy}.$$

Based on the value of $\eta$ $(0 < \eta < 1)$, one can evaluate the degree of "adiabaticity of the HFPQ process, i.e., the power of heat "sinks" from the region of the maximum heat release. Since the latter includes the zone of the highest intensity of phase transformation, i.e., the zone of the maximum hardening of steel, the value of $\eta(t)$ also shows the degree of changes in the initial steel structure by the time the prescribed final temperature $T_{\text{fin}} = T(x, y, t_i)|_{x=0,y=0}$ is reached.

As is seen from Fig. 5, until the surface is heated to a temperature of 1200–1500 K, the mean efficiency remains at a rather high level: in most variants, $\eta \approx 0.8$–$0.9$, except for the treatment modes with a lower power and treatment-zone width or with the highest field frequency where $\eta$ decreases to 0.5–0.7. With further increase in temperature of the surface layer, as was indicated above, heat fluxes related to dissipation of energy of the magnetic field drastically decrease, and heat removal from the zone of energy dissipation to surrounding metal becomes noticeable on this background: the value of $\eta$ decreases to 0.1 when only 10% of the total amount of heat released in steel due to Joule heating is spent on heating of the skin layer itself; the remaining 90% are spent on heating of deeper and lateral layers of metal, which do not experience any structural-phase transitions as a result of treatment.

Providing the maximally efficient input of energy to steel is not a self-consistent objective of the method of induction treatment; its main goal is to speed up the processes of formation of the hardened structure. The properties of the hardened structure (quenching martensite) are determined by the degree of homogenization of the high-temperature phase (austenite) formed instead of the initial phases of steel being rapidly heated. Since this process is predominantly diffusive, the main parameter of the treatment regime is the residence time of the layer in the high-temperature zone. Joint solving of Eqs. (1)–(6) allows one to determine the cross-sectional distribution of the degree of enrichment (depletion) by carbon of different phases of steel grains at an arbitrary time both at the stage of action of the HF pulse and at the stage of autoquenching.

Figure 6 shows the calculated patterns of carbon distribution over the cross section of a steel specimen; these patterns correspond to "heating–cooling" thermal cycles at different field frequencies for the following parameters: $2L_i = 4.5$ mm and $\langle W \rangle = 10^8$ W/m$^2$ (see the solid curves in Fig. 3a–c). These parameters of the treatment mode ensure rapid heating of the surface up to the melting point within the entire range of frequencies. Thus, the concentration fields in Fig. 6 differ only in time the surface was exposed to temperatures above the point of the beginning of transformation of the initial structure of steel $T > Ac_1 = 1000$ K.

In the zone of complete austenite transformation of all steel grains, the carbon concentration in those places that contained carbon-free ferrite prior to treatment gradually increases from zero to a value typical of this type of steel $\langle C \rangle = 0.45\%$ (the color in this zone changes from white to dark gray, depending on the carbon content). This zone is bounded by a very narrow region (black band) where the degree of decomposition of the pearlite component of the grain equals unity (i.e., the carbon concentration obtained by volume averaging of former pearlite regions of the steel grain reaches the maximum, or euctectoid, value of 0.8%). Outside this boundary, there is a transitional zone with a gradual decrease in both the fraction of austenite in the grain and the degree of decomposition of

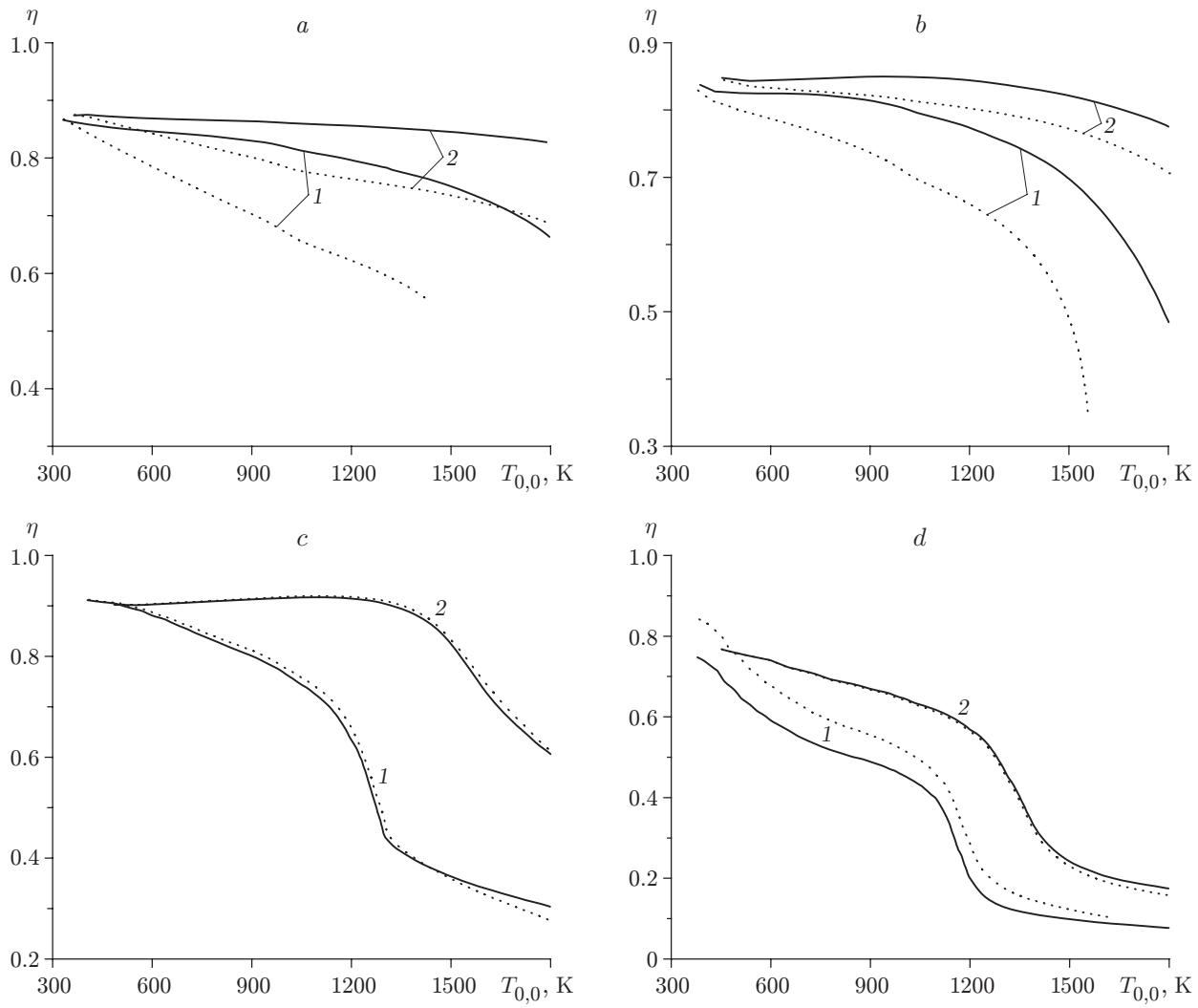


Fig. 5. Mean efficiency as a function of the surface temperature of the steel specimen for field frequencies 0.066 (a), 0.440 (b), 13.5 (c), and 40.12 MHz (d) and specific pulse power $\langle W \rangle = 10^8$ (curves 1) and $2 \cdot 10^8$ W/m$^2$ (curves 2); the heating zone width is $2L_i = 1.5$ (dotted curves) and 4.5 mm (solid curves).

pearlite. The carbon concentration in the new (austenite) phase rapidly decreases to the initial level ($C \approx 0$) with distance from the central point. The flow region that does not experience (according to our calculations) any structural-phase transitions is colored in uniform gray.

For convenience of analysis of the data obtained, the carbon distributions are superposed with the closest isotherm to the boundary of the maximum transformation of steel (i.e., zone of its maximum hardening) at the time corresponding to the end of the heating stage. This isotherm is shown by a bold dashed curve in Fig. 6. The predicted composition of steel after induction treatment at different frequencies gradually changes. For $f = 66$–$440$ kHz, an austenite layer 0.8–1 mm thick is formed on the steel-specimen surface during its heating above 1500 K; the carbon concentration in this layer is close to the maximum value of 0.45% (Fig. 6a). For $f \gg 440$ kHz, because of the shorter pulse duration, noticeable diffusion saturation by carbon to 0.2–0.3% is observed only in layers heated above 1550–1650 K (Fig. 6b–g). The maximum thickness of the hardened steel layer decreases proportionally to the field frequency from 0.4 mm for $f = 1.76$ MHz to 0.15 mm for $f = 40$ MHz. A relative reduction of the strength properties of the surface can be predicted: the ultimate strength of martensite is known to depend linearly on the carbon concentration in it [13].

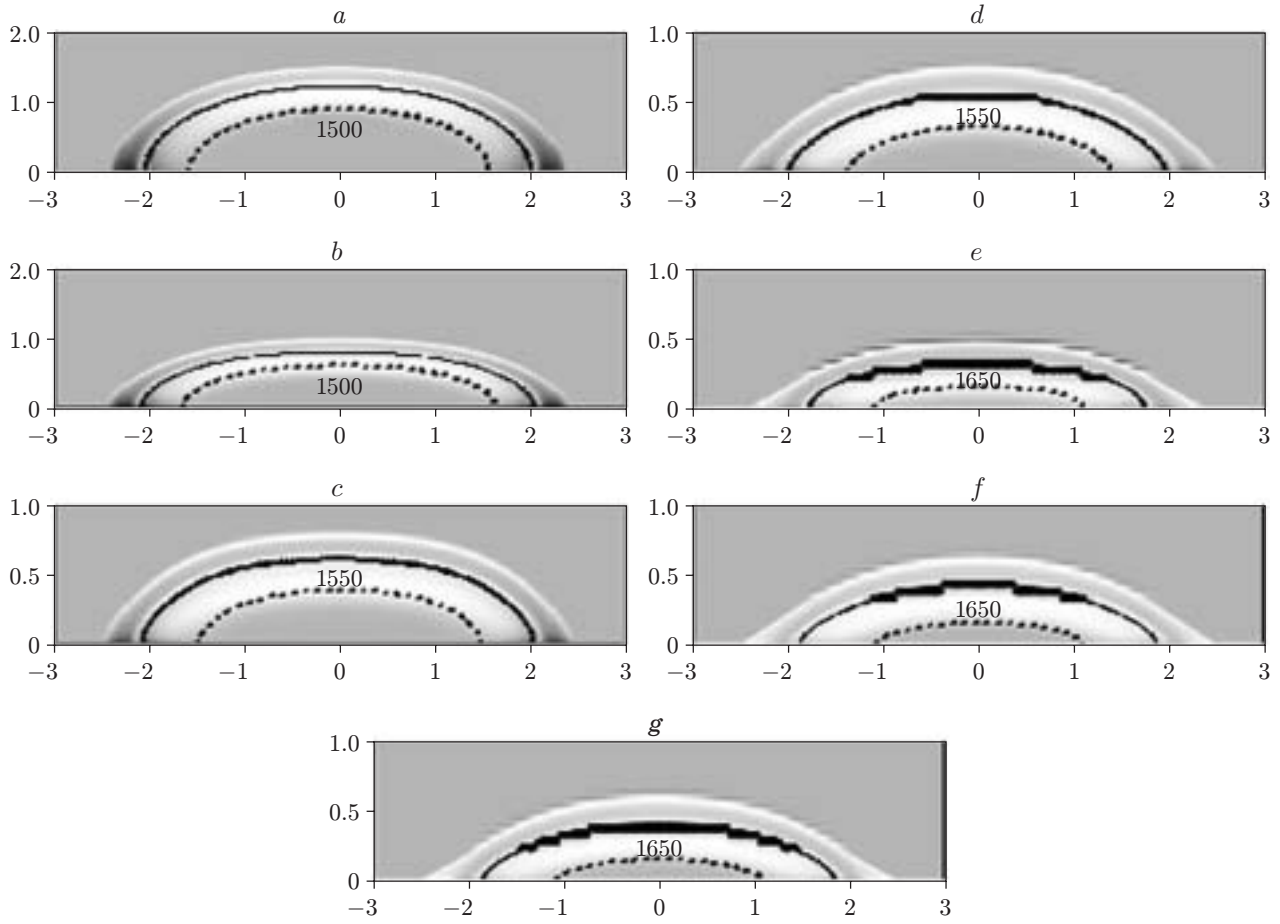


Fig. 6. Calculated distribution of carbon over the steel-specimen cross section (the distance is given in millimeters) after induction treatment at the field frequency equal to 0.066 (a), 0.440 (b), 1.76 (c), 5.28 (d), 13.5 (e), 27.1 (f), and 40.12 MHz (g). The parameters used are $2L_i = 4.5$ mm and $\langle W \rangle = 10^8$ W/m$^2$.

Similar features are also observed as the mean power of induction treatment increases to $2 \cdot 10^8$ W/m$^2$. In this case, however, a certain decrease in thickness of the austenite layer with carbon concentration higher than 0.2% is observed. Because of the shorter total duration of the thermal cycle, the lower boundary of the temperature range where diffusive saturation of austenite by carbon occurs is shifted approximately by 100 K toward higher temperatures.

**Conclusions.** The dependence of the dynamics of induction pulse heating of steel for treatment modes important in practice (with a mean specific energy flux equal to $10^8$ and $2 \cdot 10^8$ W/m$^2$ and width of the zone of pulse action of 1.5 and 4 mm) on frequency of the electromagnetic field in the interval of 0.066–40.12 MHz is analyzed. It is shown that the dynamics of heat release on the metal surface changes drastically as the field frequency increases. For moderate frequencies (66 and 440 kHz), the specific energy flux monotonically increases with increasing steel-surface temperature in proportion to the increase in its ohmic resistance; for higher frequencies (with $\langle W \rangle$ = const), magnetic properties of steel start to play the governing role in heating dynamics. At the initial stage (until temperatures of 1100–1200 K are reached), a very high heating rate ($10^5$ K/sec) is reached in a narrow layer. The energy-release intensity at the initial stage is approximately twice higher than the mean value during the entire pulse. At the next stage, the heating rate of the steel layer, which has already lost its magnetic properties, drastically decreases and stabilizes at an almost constant level, which decreases approximately to $10^3$ K/sec with increasing field frequency. The dependences of $\langle W \rangle$ and efficiency of the HF pulse on the maximum surface temperature are constructed on the basis of numerical calculations. Together with the results of numerical simulations of structural-phase transformations in the grain, these dependences allow one to choose the optimal regimes of steel hardening with different frequencies.

## REFERENCES


1. A. B. Kuvaldin, *Theory of Induction and Dielectric Heating* [in Russian], Izd. Mosk. Énerg. Inst., Moscow (1999).
2. G. Stahli, "Kurzzeit-Warmbehandlung," *Harter.-Techn. Mitt.*, **39**, 81–138 (1984).
3. D. Hinneberg, "Das HF-Impulsharten und Seine Einsatzgebiete," *Draht*, **43**, 1000–1002 (1992).
4. "Nicht tief, aber hart," *Schweizer Maschinenmarkt*, **92**, 170–173 (1992).
5. "HF-Impulsharten," *Harter.-Techn. Mitt.*, **48**, A43 (1993).
6. G. Ploger, "HF-Impulsharten — ein innovatives oberflachenharteverfahren," *Elektrowarme Intern. B*, **51**, No. 3, 110–112 (1993).
7. D. Melaab and O. Longeot, "Control of an induction heat treatment by the measure of power," *IEEE Trans. Magn.*, **29**, 1558–1561 (1993).
8. C. Chaboudez, S. Clain, R. Glardon, et al., "Numerical modeling in induction heating for axisymmetric geometries," *IEEE Trans. Magn.*, **33**, 739–745 (1997).
9. Z. Wang, W. Huang, W. Jia, et al., "3D multifields FEM computation of transverse flux induction heating for moving strips," *IEEE Trans. Magn.*, **35**, 1642–1645 (1999).
10. R. Pascal, P. Conraux, and J. M. Bergheau, "Numerical simulation of induction heating processes; comparison between direct multi-harmonic and classical staggered approaches," in: *Proc. of the 7th Int. Conf. on Advanced Computational Methods for Heat Transfer* (Halkidiki, Greece, April 22–24, 2002), WIT Press, Boston (2002), pp. 393–403.
11. V. G. Shchukin and V. V. Marusin, "Modeling of kinetics of structural-phase transformations in iron-carbon steel treated by powerful HF pulses," *Fiz. Khim. Obrab. Mater.*, No. 6, 26–39 (2000).
12. A. M. Hussein and P. P. Bringer, "Closed-formed solution for the induction heating problem with rotational symmetry," *J. Appl. Phys.*, **72**, 265–269 (1992).
13. A. El-Sesy and Z. M. El-Baradie, "Influence carbon and/or iron carbide on the structure and properties of dual-phase steels," *Mat. Lett.*, **57**, 580–585 (2002).